Generalized Synchronization of Chaos in Identical Systems with Hidden Degrees of Freedom

Atsushi Uchida,[1,2] Ryan McAllister,[1,2] Riccardo Meucci,[3] and Rajarshi Roy[1,2,4]
[1]*Department of Physics, University of Maryland, College Park, Maryland, 20742, USA*
[2]*IREAP, University of Maryland, College Park, Maryland 20742, USA*
[3]*Istituto Nazionale di Ottica Applicata, Largo Enrico Fermi, 6-50125 Firenze, Italy*
[4]*IPST, University of Maryland, College Park, Maryland 20742, USA*
(Received 22 May 2003; published 20 October 2003)

We demonstrate generalized synchronization of chaos in a two-mode laser system. The total intensity of the laser output (the sum of the individual mode intensities) is used as the drive signal. This lumped variable transmitted to the identical response system does not generate identical synchronization. Generalized synchronization is observed instead of identical synchronization because of the hidden internal degrees of freedom.

DOI: 10.1103/PhysRevLett.91.174101 PACS numbers: 05.45.Xt, 05.45.Ac, 42.65.Sf

Synchronization of chaos has been observed in many physical, chemical, and biological systems [1]. It is now widely recognized that, when the signal from one (drive) system drives a second (response) system, a great variety of synchronization phenomena may occur, including identical, phase, lag, and generalized synchronization. The last category has been observed only in very few physical systems, and it is not obviously evident when it occurs [2–4]. Generalized synchronization may have important applications in methods for noninvasive testing and monitoring of structures and materials, ranging from buildings to nanostructures, as well as in encoded communications systems.

In generalized synchronization, there is a functional relation between the dynamics of a drive and response system, but the dynamics may differ greatly in character. Generalized synchronization may be shown to exist through the predictability [2] or the existence of a functional relationship [3] between the drive and response systems. These approaches are often difficult to implement in experimental measurements, due to the presence of noise and lack of precision in measurements. When replicas or duplicates of the response system are available, the auxiliary system method has been suggested for detecting generalized synchronization [4]. One now couples two or more response systems with the drive system. If the response systems, starting from different initial conditions, display identical synchronization after transients have disappeared, we can conclude that the response signal is generally synchronized to the drive [4].

Generalized synchronization may be much more prevalent in nature than realized thus far. When systems with several degrees of freedom (e.g., fluids, neurons, lasers, chemical reagents, electronic circuits) are coupled together through only a few variables, or the drive signal is taken to be a lumped variable, the dynamics of the response system may appear quite different from that of the drive. It is possible that, under these conditions, even identical systems may display generalized synchronization, although the examples of generalized synchronization discussed in the literature consist of situations where the drive and response systems are different from each other, or of the same system operated at different parameter values [2–4]. The important question arises — can the presence of ''hidden'' internal degrees of freedom in the drive system prevent identical synchronization and result in generalized synchronization, even when identical drive and response systems are operated with parameters very close to each other, and even when they are strongly coupled? One may expect that strongly coupled identical systems with similar parameter values will display identical synchronization, if they synchronize at all [1].

We show in this Letter that generalized synchronization of chaos can occur with identical drive and response systems, with similar parameter values. In our experiment, the drive and response systems consist of a microchip laser with an optoelectronic feedback loop. The two-mode laser system provides an example where the existence of generalized synchronization can be numerically predicted and experimentally observed through the auxiliary system method. The use of a lumped variable (the total intensity) as the drive signal, and the role of the hidden interplay of longitudinal modes as a source of generalized synchronization, can be carefully examined.

Our experimental setup is shown in Fig. 1. We use a laser-diode-pumped neodymium-doped yttrium aluminum garnet (Nd:YAG) microchip laser as a laser source [5]. The total intensity of the laser output is detected by a photodiode and converted into voltage as an electronic signal. The voltage signal is fed back to an intracavity acousto-optic modulator (AOM) in the laser cavity through an electronic low pass filter with an amplifier. The loss of the laser cavity is modulated by the self-feedback signal through the AOM, which induces chaotic oscillations. The bias voltage of the AOM determines the operating point of the loss modulation. We can tune the sign (positive or negative) and the gain of the feedback signal by changing the bias voltage. Temporal waveforms of the laser output are measured by a digital oscilloscope and stored in a computer. Chaotic oscillations are

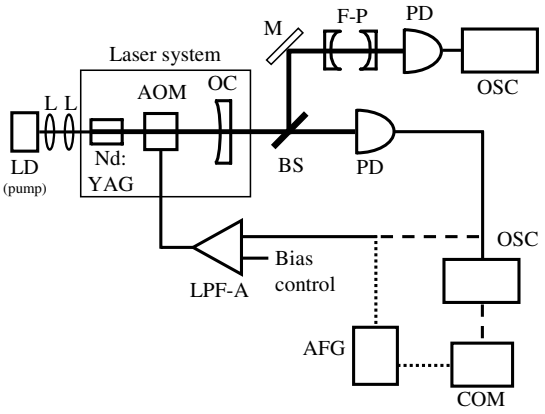

FIG. 1. Experimental setup of a diode-pumped Nd:YAG microchip laser with optoelectronic feedback. The dashed line corresponds to the closed-loop drive system, and the dotted line corresponds to the open-loop response system. AFG, arbitrary function generator; AOM, acousto-optic modulator; BS, beam splitter; COM, computer; F-P, Fabry-Perot interferometer; L, lens; LD, laser diode for pumping; LPF-A, low pass filter and amplifier; M, mirror; Nd:YAG, Nd:YAG laser crystal; OC, output coupler; OSC, digital oscilloscope; PD, photodetector.

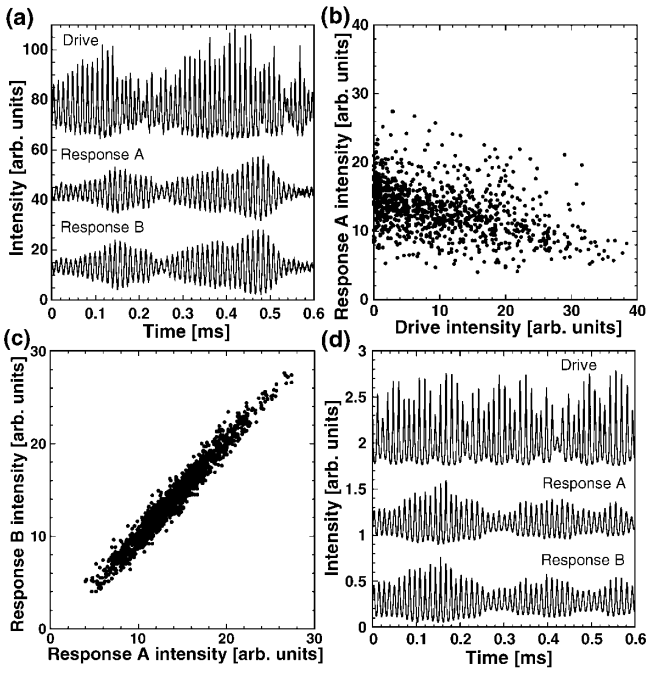

FIG. 2. (a) Temporal waveforms of experimentally measured total intensity of the drive and two response systems. (b) Correlation plots between the drive and response outputs. (c) Correlation plots between the two response outputs. (b) and (c) are obtained from (a). (d) Temporal waveforms of total intensity obtained from numerical integration of Eqs. (1)–(6).

observed under positive feedback at certain parameter regions [5]. The optical spectrum of the microchip laser is measured by a Fabry-Perot scanning interferometer. We have confirmed that two-longitudinal modes are observed in a wide range of pump power.

In order to test for synchronization, we used the same laser as a response system. The signal of the total intensity stored in the computer is used as a drive signal. The signal is sent to the AOM in the same laser cavity using an arbitrary function generator connected with the computer. In this case, the original feedback loop is disconnected (dashed line in Fig. 1) and the open loop configuration (dotted line in Fig. 1) is used for the response system. The total intensity of the laser output is detected by using the digital oscilloscope for the response system.

We expected to observe identical synchronization in this configuration because the laser systems for drive and response are identical. Typical temporal waveforms of the drive and the response are shown in Fig. 2(a). Surprisingly, there is no obvious correlation between the drive and response outputs. The correlation plot [Fig. 2(b)] shows no evidence of identical synchronization. Then we play the drive signal back to the response laser repeatedly in order to implement the auxiliary system test for generalized synchronization [4]. Two response outputs driven by the same drive signal are detected at different times, as shown in Fig. 2(a). The correlation plot between the two response outputs shows linear correlation as in Fig. 2(c). This implies that the response laser driven by the same drive signal always generates identical outputs, independent of initial conditions. Since the dynamics of the response laser are repeatable and reproducible, generalized synchronization can be stably achieved in our system.

We conducted numerical calculations in order to explain our experimental observations. Our initial simulations of the single-mode laser model presented in Ref. [5] produced only identical synchronization for identical parameter settings with strong coupling strength. Since we observed two-longitudinal laser modes with the Fabry-Perot scanning interferometer in our experiment, we used the Tang-Statz-deMars (TSD) model which includes the effect of spatial hole burning in a two-mode laser [6]. The equations are as follows:

$$\frac{dn_0}{dt} = w_0 - n_0 - \gamma_1(n_0 - n_1/2)s_1 - \gamma_2(n_0 - n_2/2)s_2, \tag{1}$$

$$\frac{dn_1}{dt} = n_0\gamma_1 s_1 - n_1(1 + \gamma_1 s_1 + \gamma_2 s_2), \tag{2}$$

$$\frac{dn_2}{dt} = n_0\gamma_2 s_2 - n_2(1 + \gamma_1 s_1 + \gamma_2 s_2), \tag{3}$$

$$\frac{ds_1}{dt} = K[\gamma_1(n_0 - n_1/2) - 1 - a\sin^2(z)]s_1, \tag{4}$$

$$\frac{ds_2}{dt} = K[\gamma_2(n_0 - n_2/2) - 1 - a\sin^2(z)]s_2, \tag{5}$$

$$\frac{dz}{dt} = -\beta[z - B - R(s_1 + s_2)], \tag{6}$$

where n_0 is the space-averaged component of population inversion density with spatial hole burning, normalized by the threshold value. n_1 and n_2 are the spatial Fourier components of population inversion density for the two-longitudinal modes. s_1 and s_2 are the normalized values of the lasing intensities for the two modes. $w_0 = 1.57$ is the optical pump parameter scaled to the laser threshold. $\gamma_1 = 1.00$ and $\gamma_2 = 0.93$ are the gain coefficients for the two modes. $K = \tau/\tau_p = 2.42 \times 10^4$, where $\tau = 0.23$ ms is the upper state lifetime and $\tau_p = 9.5$ ns is the photon lifetime in the laser cavity. Equation (6), for the voltage z applied to the AOM driver, is added to the normal TSD model to incorporate the action of an electronic low pass filter. As the photodiode does not distinguish between the two laser modes, it responds only to the total intensity $I = s_1 + s_2$ in Eq. (6). $\beta = 1.44 \times 10^2$ is the cutoff frequency of the low pass filter (corresponding to 100 kHz) [5]. The bias voltage of the AOM is represented by the normalized variable $B = 2.67$. $a = 4.0 \times 10^{-3}$ is the amplitude of the loss modulation, and the amplitude of the photodiode response is $R = 0.73$. Time for the equations is scaled by τ. All the parameters in our simulations are estimated from suitable measurements on the experimental laser system. Numerical results are calculated with the fourth-order Runge-Kutta-Gill method.

We make three copies of the set of Eqs. (1)–(6) in order to construct a system of equations simulating one drive laser with feedback and two independent response lasers, for the test of generalized synchronization. The first set appears exactly as in Eqs. (1)–(6), and Eq. (6) for the second and third sets is modified by replacing the $s_1 + s_2$ term for the response systems with the $s_1 + s_2$ from the equations of the drive system. Figure 2(d) shows the numerical results for the total intensity of drive and response lasers. The response outputs do not resemble the drive signal, whereas the two response outputs appear identical, as for the experimental measurements.

In our experiment, we found that the degree of generalized synchronization depends on the parameter mismatch between the drive and response systems. The generalized synchronization error is defined as a difference of the two temporal response waveforms: i.e.,

$$\langle e(t)\rangle = \langle |[I_A(t) - I_B(t)]/[I_A(t) + I_B(t)]| \rangle, \qquad (7)$$

where the angle brackets denote time averaging. The generalized synchronization error as a function of bias voltage detuning of the response from the drive system is shown in Fig. 3 for both the experiment [Fig. 3(a)] and numerical calculation [Fig. 3(b)]. A change of the bias voltage B of the AOM leads to a change of the laser cavity loss. It is found that there is a certain parameter range for generalized synchronization. Surprisingly, the synchronization error is minimized when the parameter is mismatched, around the bias detuning of 0.012 V, in Fig. 3(a). Therefore, the best degree of generalized synchronization is not obtained with identical matched parameters. When the bias detuning is larger, the response outputs are not repeatable and generalized synchronization is not observed.

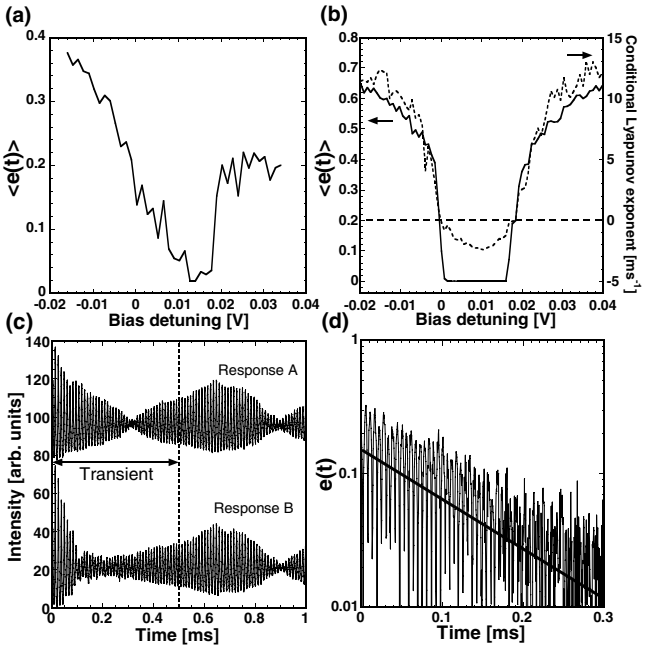

FIG. 3. Generalized synchronization error $\langle e(t)\rangle$ (solid curves) and maximal conditional Lyapunov exponent [dotted curve in (b)] as a function of the bias detuning of the response from the drive obtained in experiments (a) and simulations (b). Experimentally measured temporal waveforms (c) and time-dependent synchronization error $e(t)$ (d) showing the transient to synchronization of two responses, starting from different initial conditions. The conditional Lyapunov exponent is estimated as $\lambda_{\text{eff}} \sim -8$ ms^{-1} from the slope of the straight line fit shown in (d).

To interpret our experimental results, we calculated the maximal conditional Lyapunov exponent for generalized synchronization along the trajectory of the *response* output. The maximal conditional Lyapunov exponent for generalized synchronization as a function of the bias detuning from the drive system is also shown in Fig. 3(b). The parameter region of negative conditional Lyapunov exponents exactly matches the region of small synchronization errors. This result guarantees that the stable manifold for generalized synchronization exists in a certain parameter region as the bias voltage of the response system is changed. In Fig. 3(c), we show experimentally measured transient dynamics of the response laser from two different initial conditions. The responses begin to synchronize after about 0.5 ms. The estimated conditional Lyapunov exponent ($\lambda_{\text{eff}} \sim -8$ ms^{-1}) obtained from the plot of the time-dependent synchronization error $e(t)$ in Fig. 3(d) is of the same order of magnitude as the more precise numerical estimate in Fig. 3(b).

To examine the dynamics of the laser in greater detail, we display the temporal dynamics of each mode intensity in the simulation for the drive and response systems in Figs. 4(a) and 4(b). We calculated the cross correlation between the temporal waveforms of the two-mode

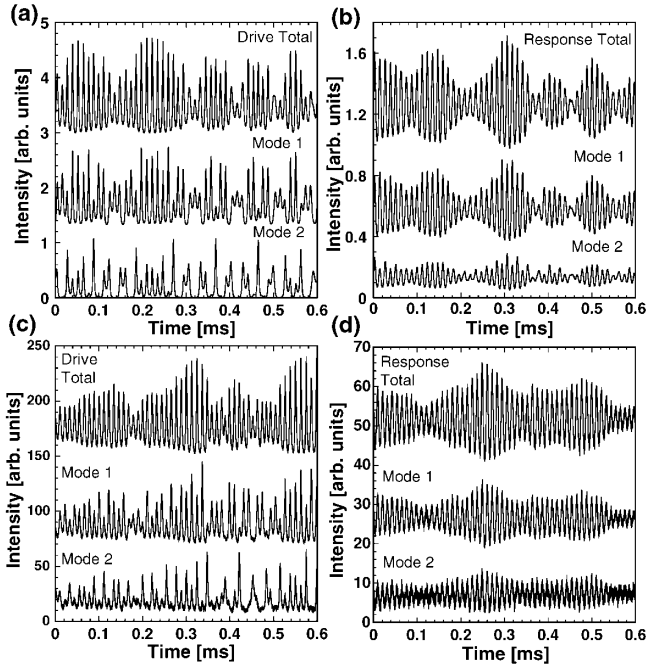

FIG. 4. Two-mode dynamics of the drive and response systems obtained in simulations [(a) and (b)] and experiments [(c) and (d)].

intensities, $C_{I_1,I_2} = \langle \Delta I_1 \Delta I_2 \rangle / (\sigma_{I_1} \sigma_{I_2})$, where $\Delta I_{1,2}$ is the deviation of the mode-1 or mode-2 intensity from the mean value and $\sigma_{I_{1,2}}$ is the standard deviation of the mode-1 or mode-2 intensity. For the specific time series, the cross correlations between the mode-1 and mode-2 intensities are estimated as 0.17 for Fig. 4(a) and 0.44 for Fig. 4(b), respectively. This implies that the temporal waveforms of the two modes in the response system are much more correlated than those in the drive system. We interpret the difference of the mode dynamics as follows: the mode-mode dynamics of the drive laser is dominated by the spatial hole burning. The lumped signal applied to the response laser does not contain any details of the individual mode dynamics. Therefore, there are internal degrees of freedom in the response laser dynamics that are not determined by the drive signal. These degrees of freedom allow a different type of temporal waveform to be produced in the response laser.

These interesting mode dynamics are confirmed in the experiment. We selected one of the two modes for transmission through a Fabry-Perot interferometer, by applying a constant voltage to its piezotransducer, which is used to change the cavity length of the interferometer. We thus detected the dynamics of one of the two modes and the total intensity simultaneously. Then we normalized the two intensities from the correlation plot and extracted the other mode dynamics by subtracting the detected mode intensity from the total intensity, as shown in Figs. 4(c) and 4(d). The calculated cross correlations of 0.27 for Fig. 4(c) and 0.71 for Fig. 4(d) also suggest that the two-mode intensities of the response system are much more correlated than those of the drive system. These experimental results accurately capture the same dynamical behavior as the numerical calculations shown in Figs. 4(a) and 4(b).

In conclusion, we have demonstrated generalized synchronization of chaos in identical two-mode microchip laser drive and response systems, although we never observed identical synchronization. In a single-mode laser model, we observed identical synchronization for similar parameter settings, whereas we never observed generalized synchronization. This result shows that the extra degrees of freedom in the multimode laser system, which are hidden in the lumped variable of the drive signal, allow generalized synchronization to be observed in identical chaotic systems.

We thank Tom Carroll, Linda Moniz, Lou Pecora, and Ira Schwartz for helpful discussions. We gratefully acknowledge support from the Office of Naval Research, Physics Division. A. Uchida thanks the Japan Society for the Promotion of Science for support. R. Meucci thanks The European Contract No. HPRN-CT-2000-158 for partial support. We are also thankful for expert technical assistance from Don Martin.

[1] L. M. Pecora and T. L. Carroll, Phys. Rev. Lett. **64**, 821 (1990); A. Pikovsky, M. Rosenblum, and J. Kurths, *Synchronization* (Cambridge University Press, Cambridge, England, 2001); S. Boccaletti, J. Kurths, G. Osipov, D. L. Valladares, and C. S. Zhou, Phys. Rep. **366**, 1 (2002).

[2] N. F. Rulkov, M. M. Sushchik, L. S. Tsimring, and H. D. I. Abarbanel, Phys. Rev. E **51**, 980 (1995); S. J. Schiff, P. So, T. Chang, R. E. Burke, and T. Sauer, Phys. Rev. E **54**, 6708 (1996); K. Yoshimura, Phys. Rev. E **60**, 1648 (1999); M. Wiesenfeldt, U. Parlitz, and W. Lauterborn, Int. J. Bifurcation Chaos Appl. Sci. Eng. **11**, 2217 (2001).

[3] R. Brown, Phys. Rev. Lett. **81**, 4835 (1998); J. Arnhold, P. Grassberger, K. Lehnertz, and C. E. Elger, Physica (Amsterdam) **134D**, 419 (1999); C. L. Goodridge, L. M. Pecora, T. L. Carroll, and F. J. Rachford, Phys. Rev. E **64**, 026221 (2001); V. Afraimovich, A. Cordonet, and N. F. Rulkov, Phys. Rev. E **66**, 016208 (2002); B. R. Hunt, E. Ott, and J. A. Yorke, Phys. Rev. E **55**, 4029 (1997).

[4] H. D. I. Abarbanel, N. F. Rulkov, and M. M. Sushchik, Phys. Rev. E **53**, 4528 (1996); L. Kocarev and U. Parlitz, Phys. Rev. Lett. **76**, 1816 (1996); K. Pyragas, Phys. Rev. E **54**, R4508 (1996); D. Y. Tang, R. Dykstra, M. W. Hamilton, and N. R. Heckenberg, Phys. Rev. E **57**, 5247 (1998); A. Uchida *et al.*, Phys. Rev. E **68**, 016215 (2003).

[5] R. Meucci, R. McAllister, and R. Roy, Phys. Rev. E **66**, 026216 (2002); R. McAllister, R. Meucci, D. DeShazer, and R. Roy, Phys. Rev. E **67**, 015202(R) (2003).

[6] C. L. Tang, H. Statz, and G. deMars, J. Appl. Phys. **34**, 2289 (1963).